A number of interlinking microbial pathways contribute to N-loss in OMZs and control the corresponding production of biogenic N_2. Whereas heterotrophic denitrification (HDN; $NO_3^- \rightarrow N_2$ via NO_2^-) was canonically viewed as dominant, important roles are now ascribed to the chemosynthetic anammox process (ANM; $NO_2^- + NH_4^+ \rightarrow N_2$; Kuypers et al., 2003) as well as dissimilatory nitrate reduction to ammonia (DNRA; $NO_3^- \rightarrow NH_4^+$ via NO_2^-; Lam et al., 2009). Recent studies disagree as to whether HDN or ANM is the dominant process for producing biogenic N_2 (Ward et al., 2009; Bulow et al., 2010; Hamersley et al., 2007) and it remains unclear if these differences are the result of regional contrasts, time space^{-1} heterogeneity, or methodology (Voss and Montoya, 2009). Coupling these pathways can result in variable stoichiometry between NO_3^- removal and N_2 production provided there is an allochthonous supply of NH_4^+. However, recent comparison between NO_3^- deficits and biogenic N_2 in several OMZs are consistent with traditional stoichiometries (e.g. Chang et al., 2010), providing no evidence for allochthonous ammonium supporting the N-loss processes in the open ocean OMZs. These microbial processes do vary in their environmental sensitivities, such as threshold O_2 concentration (Kalvelage et al., 2011), so that knowledge of variability in their presence and activity is required for modeling and prediction of response to future global change.

Stable N isotope distributions in the ocean are also greatly influenced by N-loss processes (variations in $^{15}N/^{14}N$ are expressed in the $\delta^{15}N$ notation as ‰ difference from the ratio for atmospheric N_2). Dissimilatory NO_3^- reduction to NO_2^- is known to produce both strong N as well as O isotopic fractionation (Granger et al., 2008) leaving residual seawater NO_3^- enriched and the product NO_2^- depleted in ^{15}N and ^{18}O (Casciotti and McIlvin, 2007; fractionation factor, ε □ 25 ‰). Presumably because ^{15}N-depleted N

High precision N_2/Ar for detection of biogenic N_2 and δ^{15}N-N_2 were determined on septum sealed samples using on-line gas extraction system coupled to a multicollector IRMS (Bristow et al., 2012TS1). These data were produced by removing O_2 in the samples prior to introduction into the mass spectrometer to avoid artifacts associated with varying N_2/O_2 (Devol et al., 2006). In terms of calculated biogenic N_2, certainty is on the order of ± 1 µmol kg^{-1}. δ^{15}N-N_2 data were acquired during the same analytical sessions with a certainty of ± 0.05 ‰. Publicly available satellite data for sea surface chlorophyll (SSC) are from the NASA Giovanni website (http://gdata1.sci.gsfc.nasa.gov) and sea level anomaly (SLA) are from the AVISO website (http://www.aviso.oceanobs.com).

3 Results

3.1 Properties maps of Peru OMZs

For context, relevant biogeochemical properties are mapped along a constant density (isopycnal) surface to highlight the effects of non-conservative, N-cycling processes (Fig. 1). The chosen isopycnal density corresponding to $\sigma_\theta = 26.3\,\mathrm{kg\,m^{-3}}$ varied between 100 and 170 m depth and was located vertically near the top of the minimum O_2 layer of the water column. South of 7 to 10° S, O_2 concentrations on this isopycnal surface were generally low enough to enable N-loss processes (< 3 µmol kg^{-1}; Fig. 1a) consistent with prior observations (Codispoti and Christensen, 1985). Southward intensification of the OMZs along its northern boundary is associated with the poleward flow of the Peru Undercurrent (PUC) partly sourced in the lower equatorial undercurrent (Strub et al., 1987), comprising both the OMZs core and the primary source of upwelled waters in this region. Onset of dissimilatory NO_3^- reduction in the OMZs is marked by the pronounced appearance of NO_2^-, which is both an intermediate for HDN and DNRA, as well as a substrate for ANM (Fig. 1b). For most of the open ocean portion of the Peru OMZs, maximal $[NO_2^-]$ is < 5 µmol kg^{-1}. Net N-loss as a consequence of NO_3^- conversion to N_2 gas has been previously estimated using N-deficit calculations based on anomalies in the oxidized forms of N relative to the Redfield proportionality with PO_4^{-3} (Devol et al., 2006):

$$N^{\square} = NO_3^- + NO_2^- - 16 \times PO_4^{-3} \tag{1}$$

The N-deficit, $N^{\square}$, is similar to the N* formulation (Gruber and Sarmiento, 1997) but without the latter's constant offset (Appendix A). NH_4^+ is not included as its concentration has been observed to be very low to non-detectable throughout much of our study area, particularly seaward of the shelf. PO4]TJ/F26 7.572 Tf 194.84 4.295 Td[( )]TJ/F44 7.572 Tf 0 -(kg)6 Td[(2)]TJ/95

South of 7 to 10° S, $N^{\square}$ decreases from −5 to ol et in1t9kgTf 8.7156 Td6es are maTf 6.404 3.331 Td24.46825(to)π

Fig. 2. Depth profiles for N-loss indicators at Station 7 showing extreme values as compared to nearby, shoreward Station 9. OMZs ($O_2 < 5$ µmol kg^{-1}) indicated as a shaded depth interval (see also Fig. 3). **(A)** NO_2^- and N-deficit (N^*) concentration profiles (µmol kg^{-1}). **(B)** Profiles for $\delta^{15}NO_3^-$ (‰ relative atmospheric N_2). **(C)** Crossplot of the δ^{18}O vs. the δ^{15}N of NO_3^-. **(D)** Rayleigh plot of $\delta^{15}NO_3^-$ vs. the ln of the residual NO_3^- fraction assuming the NO_3 concentration prior to removal is approximated as $16 \times [PO_4^{-3}]$. The inverse slope estimates the fractionation effect (ε) at ∼ 17 ‰.

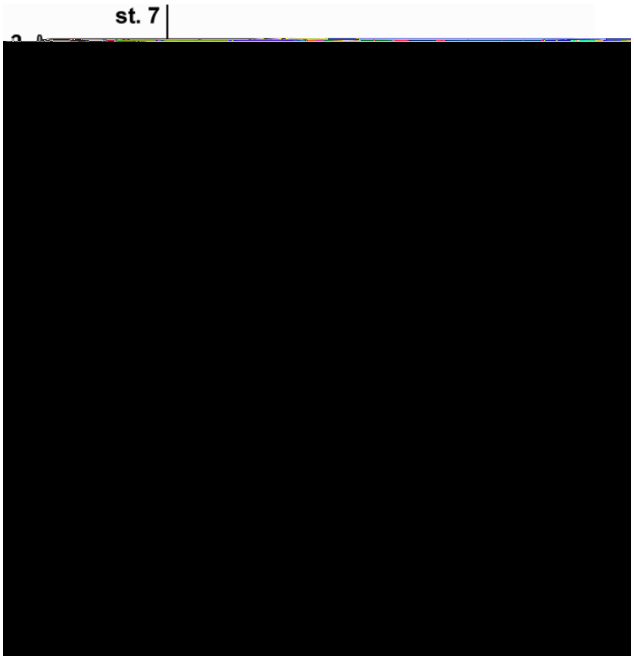

Fig. 3. Property distribution section off the Peru coast. **(A)** O_2 concentration (µmol kg^{-1}; color shading) and σ_θ (contour lines) sections at 12 and 14° S latitude (see station positions in Fig. 1). Station 7 is part of the 12° S section and its position is marked. **(B)** Corresponding N^*

and 2). The highest measured values of δ^{15}N and δ^{18}O for OMZs NO_3^- that we are aware of, are also observed at this station reaching 40 and 34 ‰ (Fig. 2b). In contrast, ocean-wide $\delta^{15}NO_3^-$ averages are near 5 and 2 ‰, respectively (Sigman et al., 2009). At our other Peru OMZs stations, maximal $\delta^{15}NO_3^-$ is typically ∼ 15 ‰ and values as high as 24 ‰ have been reported from other OMZs (Altabet et al., 1999). Although the extrema are relatively shallow (100 m), these N-loss indicators at Station 7 extend broadly over the water column down to 400 m depth, corresponding to the layer of lowest O_2 concentration (Figs. 2, 3). Sections for N^* and [NO_2^-] on a E–W transect at 12° S also confirm Station 7 to be distinct as compared to neighboring stations, particularly with respect to the greater vertical extent of maxima. In con-

3.3 Biogenic N_2

The amount of biogenic N_2 production resulting from N-loss processes (HDN or ANM) can be estimated from high precision N_2/Ar determinations (Chang et al., 2010). Biogenic N_2 production increases the measured N_2/Ar ratio over the value predicted from equilibration with the atmosphere at in situ temperature and salinity. Deviations from equilibrium N_2/Ar ratios are also known to arise from physical processes such as bubble injection in water mass formation regions. Our data are adjusted as previously described to account for this (Chang et al., 2010), allowing estimation of an "excess" N_2 concentration due to biological processes. Biogenic N_2 concentrations below the oceanic mixed layer can also be predicted using Richards stoichiometry (Richards, 1965) which takes into account nitrogen originating from the breakdown of OM that does not appear as NH_4^+ and is assumed to be also converted to N_2 (Appendix A):

$$N_{2\ \mathrm{biogenic}}{}^{\square}\ \text{as}\ \mu\mathrm{mol\,kg^{-1}}\,N_2{}^{\square} = {}^{\square}N^{\square}_{\mathrm{source\ waters}} - N^{\square}_{\mathrm{OMZs}}{}^{\square} \times 0.5 \quad (2)$$

Measured biogenic N_2 concentrations throughout the OMZs at Station 7 (70 to 400 m) closely follows concentrations predicted from the $N^{\square}$ data (Fig. 4a) suggesting that NO_3^- removal is well balanced by biogenic N_2 production even for these relatively high OMZs values. However, measured biogenic N_2 concentrations in the oxycline of Station 7, above the core of the OMZs (50 to 70 m), are twice as high as the values predicted from $N^{\square}$ and > 20 times our analytical uneration of any synoptic mesoscale variability. As observed from satellite images, both anticyclonic and cyclonic eddies are important and persistent features of the circulation of this coastal upwelling system, as well as of the eastern tropical South Pacific as a whole (Chaigneau et al., 2008). Off Peru, coherent eddies are typically formed along the coast and propagate westward at 3 to 6 km d^{-1} and have a mean eddy lifetime of □ 1 month. Their mean radius is 80 km, increasing equatorward due to the increasing Rossby Radius of Deformation. Eddies are most frequently observed off Chimbote (9° S) and south of San Juan (15° S), north and south

average δ^{15}N for biogenic N_2 within the OMZs at Station 7 is □ −1 ‰ and thus only 6 ‰ less than the oceanic average $\delta^{15}NO_3^-$. When applied to global N isotope budgets, the resulting lower effective fractionation effect for OMZs N-loss also implies that OMZs account for a larger portion of overall oceanic N-loss than previously thought (Altabet, 2007) as well as an oceanic fixed-N budget closer to balance.

The impact of coastal mesoscale eddies on OMZs N-loss processes reported here is unlikely to be restricted to the waters off Peru, especially as the number of eddies can be greater in the other large OMZs, off Mexico and in the Arabian Sea (Chelton et al., 2011). However, OMZs also extend geographically far beyond the region of direct influence of coastal eddies, especially the one off Mexico (Codispoti and Richards, 1976). In oligotrophic open ocean regions, mesoscale eddies in particular are recognized as enhancing the vertical flux of nutrients and primary productivity (McGillicuddy and Robinson, 1997; McGillicuddy et al., 1998). Since most mesoscale eddies have recently been characterized as "non-linear" and capable of advecting water parcels, they have even greater potential for biogeochemical impact on the subsurface ocean (Chelton et al., 2011). Open-ocean eddies may thus produce similar "hotspots" for microbially mediated N-loss even in portions of OMZs that are distant from productive coastal waters.

Appendix A

A1 Use of N' to estimate NO_3^- removal and production of biogenic N

Outside of OMZs, NO_3^- generally varies in stoichiometric proportion with PO_4^{-3} and O_2 as originally observed by Redfield (Redfield, 1958). Negative deviations in $[NO_3^-]$ from values expected from these proportions has been termed the NO_3^- deficit and is used to estimate net removal and production of biogenic N_2 in OMZs (Devol et al., 2006). The commonly used N* ($= [NO_3^-] - 16 \times [PO_4^{-3}] + 2.9$; Gruber and Sarmiento, 1997) assumes NO_3^- as the only form of dissolved inorganic N, uses the Redfield N : P ratio, and applies an offset of 2.9 that allows for global average N* to be 0. We have used a modification of N* ($N' = NO_3^- + NO_2^- - 16 \times PO_4^{-3}$), which takes into account NO_2^-, which can be found at significant concentrations in OMZs, and forgoes the global offset as not being relevant regionally. N' slightly overestimates actual NO_3^- removal (a more negative N') because of PO_4^{-3} release from organic matter breakdown by about 16 % (Devol et al., 2006). Accordingly, biogenic N_2 ($N_{2\ \mathrm{biogenic}}$) assuming equivalence with NO_3^- removal as well as Richards' stoichiometry (1.71 NO_3^- : 1 N_2; Richards,

was provided by the Deutsche Forschungsgemeinschaft-supported project SFB-754 (www.sfb754.de). The R/V *Meteor* M77/3 and M77/4 Pacific cruises were granted by the DFG and the crews and captain of R/V *Meteor* are thanked for their help during cruises M77/3 and M77/4.

Edited by: B. Dewitte

References

Altabet, M. A.: Constraints on oceanic N balance/imbalance from sedimentary ^{15}N records, Biogeosciences, 4, 75–86, doi:10.5194/bg-4-75-2007, 2007.

Altabet, M. A., Murray, D. W., and Prell, W. L.: Climatically linked oscillations in Arabian Sea denitrification over the past 1 m.y.: Implications for the marine N cycle, Paleoceanography, 14, 732–743, doi:10.1029/1999PA900035, 1999.

Altabet, M. A., Higginson, M. J., and Murray, D. W.: The effect of millennial-scale changes in Arabian Sea denitrification on atmospheric CO_2, Nature, 415, 159–162, doi:10.1038/415159a, 2002.

Brandes, J. A. and Devol, A. H.: Isotopic fractionation of oxygen and nitrogen in coastal marine sediments, Geochim. Cosmochim. Ac., 61, 1793–1801, doi:10.1016/S0016-7037(97)00041-0, 1997.

Brandes, J. A. and Devol, A. H.: A global marine-fixed nitrogen isotopic budget: Implications for Holocene nitrogen cycling, Global Biogeochem. Cy., 16, 1120–1134, doi:10.1029/2001GB001856, 2002.

Bruland, K. W., Rue, E. L., Smith, G. J., and DiTullio, G. R.: Iron, macronutrients and diatom blooms in the Peru upwelling regime: brown and blue waters of Peru, Mar. Chem., 93, 81–103, doi:10.1016/j.marchem.2004.06.011, 2005.

Bulow, S. E., Rich, J. J., Naik, H. S., Pratihary, A. K., and Ward, B. B.: Denitrification exceeds anammox as a nitrogen loss pathway in the Arabian Sea oxygen minimum zone, Deep-Sea Res. Pt. 1, 57, 384–393, doi:10.1016/j.dsr.2009.10.014, 2010.

Carpenter, E. J., Harvey, H. R., Fry, B., and Capone, D. G.: Biogeochemical tracers of the marine cyanobacterium *Trichodesmium*, Deep-Sea Res. Pt. 1, 44, 27–38, doi:10.1016/S0967-0637(96)00091-X, 1997.

Casciotti, K. L. and McIlvin, M. R.: Isotopic analyses of nitrate and nitrite from reference mixtures and application to Eastern Tropical North Pacific waters, Mar. Chem., 107, 184–201, doi:10.1016/j.marchem.2007.06.021, 2007.

Chaigneau, A., Gizolme, A., and Grados, C.: Mesoscale eddies

McGillicuddy, D. J., Robinson, A. R., Siegel, D. A., Jannasch, H. W., Johnson, R., Dickeys, T., McNeil, J., Michaels, A. F., and Knap, A. H.: Influence of mesoscale eddies on new production in the Sargasso Sea, Nature, 394, 263–266, doi:10.1038/28367, 1998.

McIlvin, M. R. and Altabet, M. A.: Chemical conversion of nitrate and nitrite to nitrous oxide for nitrogen and oxygen isotopic analysis in freshwater and seawater, Anal. Chem., 77, 5589–5595, doi:10.1021/ac050528s, 2005.

Naqvi, S. W. A., Jayakumar, D. A., Narvekar, P. V., Naik, H., Sarma, V., D'Souza, W., Joseph, S., and George, M. D.: Increased marine production of N_2O due to intensifying anoxia on the Indian continental shelf, Nature, 408, 346–349, doi:10.1038/35042551, 2000.

Redfield, A. C.: The biological control of chemical factors in the environment, Am. Sci., 46, 205–221, 1958.

Richards, F. A.: Anoxic basins and fjords, in: Chemical Oceanography, edited by: Riley, J. P. and Skirrow, G., Academic Press, London, 611–643, 1965.

Ryabenko, E., Altabet, M. A., and Wallace, D. W. R.: Effect of chloride on the chemical conversion of nitrate to nitrous oxide for $\delta^1$5N analysis, Limnol. Oceanogr. Methods, 7, 545–552, 2009.

Ryabenko, E., Kock, A., Bange, H. W., Altabet, M. A., and Wallace, D. W. R.: Contrasting biogeochemistry of nitrogen in the Atlantic and Pacific oxygen minimum zones, Biogeosciences 9, 203–215, 10.5194/bg-9-203-2012, 2012.

Sigman, D. M., Granger, J., DiFiore, P. J., Lehmann, M. M., Ho, R., Cane, G., and van Geen, A.: Coupled nitrogen and oxygen isotope measurements of nitrate along the eastern North Pacific margin, Global Biogeochem. Cy., 19, GB4022, doi:10.1029/2005GB002458, 2005.

Sigman, D. M., DiFiore, P. J., Hain, M. P., Deutsch, C., Wang, Y., Karl, D. M., Knapp, A. N., Lehmann, M. F., and Pantoja, S.: The dual isotopes of deep nitrate as a constraint on the cycle and budget of oceanic fixed nitrogen, Deep-Sea Res. Pt. 1, 56, 1419–1439, doi:10.1016/j.dsr.2009.04.007, 2009.

Stramma, L., Johnson, G. C., Sprintall, J., and Mohrholz, V.: Expanding oxygen-minimum zones in the tropical oceans, Science, 320, 655–658, doi:10.1126/science.1153847, 2008

Stramma, L., Visbeck, M., Brandt, P., Tanhua, T., and Wallace, D.: Deoxygenation in the oxygen minimum zone of the eastern tropical North Atlantic, Geophys. Res. Lett., 36, L20607, doi:10.1029/2009gl039593, 2009.

Strub, P. T., Allen, J. S., Huyer, A., and Smith, G. J.: Seasonal cycles of currents, temperatures, winds, and sea level over the northeast Pacific continental shelf: 35°

Remarks from the Typesetter

TS1